

Photocatalytic degradation of cefazolin over TiO₂ coated on the fixed bed under UV_C and solar

Mahdieh Masihpour^a, Hamidreza Nassehinia^b, Ayat Rahmani^{c,*}

^aEnvironmental Health, Department of Environmental Health, Semnan University of Medical Sciences, Semnan, Iran, Tel. +982335220132; email: m-masihpour68@yahoo.com (M. Masihpour)

^bResearch Center for Health Sciences and Technologies, Semnan University of Medical Sciences, Semnan, Iran, Tel. +982335220132; email: hamidrezanassehi@gmail.com (H. Nassehinia)

^cResearch Center for Health Sciences and Technologies, Semnan University of Medical Sciences, Semnan, Iran, Tel. +989333900151; email: ayat_rahmani@yahoo.com (A. Rahmani)

Received 10 February 2019; Accepted 16 November 2019

ABSTRACT

The presence of antibiotics in the environment especially in aqueous environments is a major warning about health and the environment. In this study, the photocatalytic degradation of cefazolin antibiotics was studied on the TiO₂ nanoparticles coated on the fixed bed, which was treated in two light sources including UV_C (250 nm) and natural solar. The effects of the operational parameters such as the initial concentration of the cefazolin and two light sources were examined and compared in both systems. Characterization of the TiO₂ samples was performed by field emission scanning electron microscopy, X-ray diffraction, UV-VIS spectrophotometer, and surface area Brunauer–Emmett–Teller measurements. The highest photocatalytic activity for the degradation of cefazolin was obtained for the TiO₂/UV_C and 99% efficiency in 120 min. Also, the highest photocatalytic activity for the degradation of cefazolin was obtained for the direct TiO₂/solar and 84% efficiency in 120 min. The photocatalytic degradation reaction of cefazolin was monitored by high performance liquid chromatography, total oxygen demand, and gas chromatography–mass spectrometry (GC-MS) analyses. The GC-MS analysis results indicate that degradation of cefazolin occurs through by-products thiocarbamide acid, thiadiazole, propanone, tetrazole, and dihydrothiazine ring cleavages followed by subsequent reactions with OH radicals. Finally, these substances become more stable and turn to mineral materials containing sulfate nitrate, and ammonia.

Keywords: Cefazolin; Photocatalytic degradation; Solar; TiO₂; UV_C

1. Introduction

Among all the pharmaceuticals, water, and wastewater contaminants, antibiotics play an important role because of their high consumption in human medicine and veterinary. This issue has stirred concern about environmental pollution [1]. The concentration of these materials has been reported to be in the range of several nanograms per liter to a gram per liter [2,3]. A characteristic example of antibiotics is cefazolin. This semisynthetic antibiotic is used to treat common

bacterial infections. For solar play, materials active in the visible range are more desirable. [4].

Of various treatment techniques to purify the wastewater containing pharmaceutical compounds, the advanced oxidation processes have been proved more feasible in comparison with other techniques such as activated carbon adsorption, air stripping, and reverse osmosis because these techniques only transfer the contaminants from one phase to another without destroying them [5,6]. Photocatalysis was the acceleration of a photoreaction with the presence of the catalyst. When a semiconductor was irradiated through

* Corresponding author.

above bandgap illumination, the radiation energy was absorbed and electrons were promoted since the valence band to the conduction band giving increase to the formation of electron–hole pairs. If the charge carriers reach the semiconductor/ water interface they may participate in redox reactions. The reactive oxygen species are very active, indiscriminate oxidants, especially the hydroxyl radical [7,8]. The reactive oxygen species can not only destroy an enormous variety of chemical contaminants in water but also reason fatal damage to microorganisms. The photocatalytic properties of numerous semiconductors had been investigated (TiO_2 , ZnO , Fe_2O_3) [9,10]. Between these, the most commonly used for water treatment applications are titanium dioxide (TiO_2) and zinc oxide (ZnO). TiO_2 and ZnO were the wideband semiconductors whose bandgap energy of 3.2 and 31.3 eV corresponds to photons of wavelength shorter than 400 nm. If the interest is the solar application, materials active in the visible range are desirable [11–15].

The purpose of this study is to assess the feasibility of the photocatalytic degradation of cefazolin in the presence of fixed-bed TiO_2 . For this purpose, TiO_2 nanoparticles were coated on a fixed bed treated with two light sources; that is, UV_C (250 nm) and solar light. Characterization of the fixed bed TiO_2 samples was performed by field emission scanning electron microscopy (FE-SEM), X-ray diffraction (XRD), UV-VIS spectrophotometer, and surface area Brunauer–Emmett–Teller (BET) measurements. The degradation reaction was also followed by high performance liquid chromatography (HPLC) and gas chromatography–mass spectrometry (GC-MS) analyses.

2. Materials and methods

2.1. Materials

In this research, a cefazolin antibiotic with 95% purity was prepared from Razi Company in Iran. Other materials used in the experiments, including hydrofluoric acid, methanol, acetonitrile, H_2O_2 , and water grade HPLC, were purchased from Merck, Germany.

2.2. Preparation of TiO_2

The TiO_2 nanoparticle obtained from the XRD analysis showed an average particle diameter of 21 nm, and 79% anatase and 21% rutile phases in a molecular state. The purity of this nanoparticle is 99.5% and its effective surface is $51.1 \text{ m}^2/\text{g}$. In this research, the coating method was applied on the surface of a glass substrate. First, to create a higher effective surface on the glass, the glass surface was placed in contact with 30% hydrofluoric acid for 1 h. Next, the surface of the substrate was completely washed with distilled water. Afterward, the glass substrate was contacted with NaOH with the normality of 1. Subsequently, for making the TiO_2 solution, the TiO_2 powder with 99.5% purity and the solution with 3% TiO_2 was prepared. In the next step, the solution is placed in an ultrasonic apparatus at 50°C for 90 min to obtain a homogeneous mixture. After distributing this homogeneous suspension on the glass surface, we place it at a normal temperature for 3–4 h. Following this period, the water remaining on the residual glass surface is

removed and the sample is placed at a normal temperature for 24 h to dry again. After this step, the glass is placed in the furnace for 1 h and a half and the temperature gradually increases from 50°C to 500°C to calcify the nanoparticles on the substrate surface [16].

2.3. Construction of the reactor

The batch reactor used in this study is a closed system schematically shown in (Fig. 1). The light source in the reactor is a UV_C lamp with an average pressure and a nominal power of 18 W/h and a length of 30 cm, which is placed exactly in the center of a mirror cylinder used as the reactor cap. In reactor 2, the solar light is used as a light source in the photocatalytic process.

2.4. Characterization techniques

To investigate the physical and chemical properties and the porosity of materials, scanning electron microscopy and XRD was utilized [11]. To measure the light absorbance of the TiO_2 nanoparticle both in powder and coated form, the UV-VIS spectrophotometer 2601UV model at wavelengths of 200–1,000 nm was used.

2.5. Experiments

In this study, a stock 1,000 mg/L antibacterial powder of cefazolin was used to prepare the test solutions. The treatment periods of 120, 90, 60, 30, 20, 15, 10, 5, and 0 min were investigated in this work. HPLC was used to measure residual concentrations in wastewater. The solutions were prepared as standard concentrations (i.e., 5, 10, 15, 20, and 25 mg/L) from the stock sample to obtain peak time and a calibration curve. Then, different concentrations of cefazolin antibiotics were prepared and a sample with a constant concentration of 10 mg/L with a volume of 1 L was added to the reactor. After UV_C emission at a wavelength of 250 nm at specified times, the sample was placed in the HPLC apparatus for analysis [17]. The cefazolin antibiotic concentration is measured by a standard HPLC apparatus with a C18 column and methanol and water moving phase (30:70 v/v) [18]. All experiments were performed in laboratory conditions at $25^\circ\text{C} \pm 2^\circ\text{C}$.

2.6. GC-MS analysis

To determine the degradation process of the contaminants and intermediate materials in the refined solution, the residual reactor samples were used in the GC-MS device. The samples in this section were tested at 30, 90, and 120 min intervals. For sample preparation 9 cc of filtered sample along with 5 cc of methanol with gas chromatography (GC) grade and 1 cc of chloroform were mixed in falcon tube made of polyethylene, and placed in a centrifuge machine with 3,500 rpm for 30 min; then, 1 cc of the solution in the separated phase was removed from the surface and injected into the GC-MS device.

2.7. Reaction kinetics

In this study, (Eq. (1)) was used to calculate the reaction kinetics.

$$\ln \frac{C}{C_0} = -kt \quad (1)$$

In this equation, C_0 is the initial concentration and C is the concentration of the wastewater. t is the solution contact time in the reactors and k is the reaction speed constant. In this study, Eq. (2) was used to calculate the synergistic properties of the reactions [11].

$$\text{Syn} = \frac{\frac{\text{TiO}_2}{\text{UV}_c} - \text{UV}_c}{\frac{\text{TiO}_2}{\text{UV}_c}} \quad (2)$$

2.8. Total oxygen demand test

The total oxygen demand (TOC) test was used to control the process of mineralization of the samples and to determine the ingredients of the organic matter of the wastewater. For this purpose, 10 cc of the sample was taken and after injecting 0.1 cc HCl 1 normal, the NPOC method (non purgeable organic carbon) content of the sample was measured by the TOC meter machine at 800°C. The model of the device was Jena-C3100 made in Germany [19].

2.9. Boltzmann transport equation test

The Boltzmann transport equation machine was used to determine the effective surface of nanoparticles in both powdered forms and after coating conditions. In this experiment, the TiO_2 sample was first prepared in powder form before coating, and then the nanoparticles after coating were prepared to test the effective surface area.

2.10. Solar experiment

All experiments were performed under natural solar radiation in Damghan, an Iranian city located in 44°63' to 63°18' E and 25°3' to 39°47' N, which is a very good position to receive solar energy. Tests started at 11 a.m. and finished at 15 p.m. local time. Solar and UV irradiance was measured with a global UV radiometer (295–385 nm UV and 400–1,500 nm Solar, Model HAGNER, Sweden). The initial temperature of all samples was about 20°C.

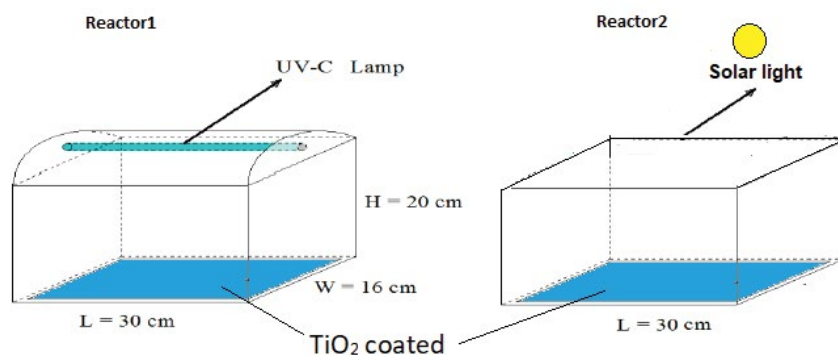


Fig. 1. Schematic of the reactors used in this study.

3. Results and discussion

3.1. Characterization of the nanocatalyst

The results of the XRD of powdered nanoparticles and the layer coated on the glass substrate are shown in (Fig. 1).

In XRD results, both molecular phases of nanoparticles are calculated to be 79% anatase and 24% rutile. Also, the anatase peak number (101) has a large consistency with the angle before the coating. The comparison of the anatase and rutile phase before and after the nanoparticle coating showed that the coating process, which was carried out at 550°C in the vacuum furnace, did not change the structure of the nanoparticle (Fig. 2). The results of the BET test presented in (Table 1) show that during the coating process, the size of nanoparticle crystals has increased from 21 nm in a powdery state to 35 nm after the coating. Changing the size of the nanoparticle crystal can be caused by the high calcification on the surface of the glass substrate.

In (Fig. 3a), FE-SEM shows the surface of the glass substrate before coating, which caused the contact of the substrate with hydrofluoric acid and corrosion on the glass surface to provide a suitable substrate for the nanoparticle coating. (Fig. 3b), shows the substrate after coating that the nanoparticle is uniformly distributed over the entire surface.

Moreover, Fig. 3c shows the size of the particles in the indicated layer. After the coating process, the size of the crystals is larger than the powdery state. The effective surface

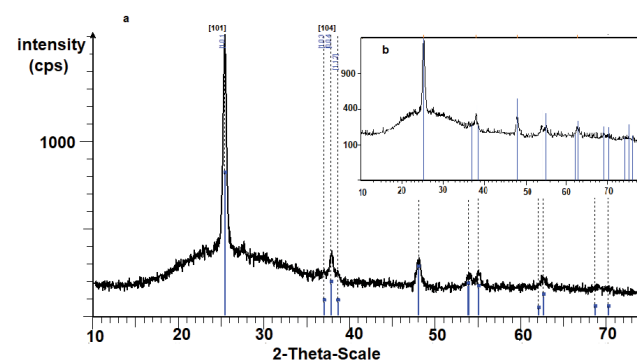


Fig. 2. XRD diffractograms for TiO_2 samples after coating (a) and before coating (b).

of the nanoparticle is 51.1 m²/g in powder form (Table 2). After the coating, the effective surface of nanoparticles decreased to 47.3 m²/g, probably due to the calcification process during the coating process [11]. In this study, the UV absorption rate by nanoparticles was investigated at a wavelength range of 200–1,000 nm by UV-vis diffuse reflectance

spectroscopy. The results of this analysis show that the highest UV absorption is at 250 nm wavelength in the UV_C wavelength range. The nanoparticle also has a maximum absorption rate at wavelengths of 320–360 nm, which are located in the UV_A wavelength range. This nanoparticle has a very low absorption at wavelengths higher than 400 nm, which is in the range of the visible light of the sun [4].

Table 1

Crystallite sizes, surface areas, bandgap energies E_g and absorption wavelengths for the TiO₂ samples

	TiO ₂	TiO ₂ (coating)
BET, m ² /g	51.1	47.8
Crystal size, nm	21	35
Purity, %	99.5	99.4
E_g , eV	3.02	3
UV _C (max absorption), nm	250	250
Solar light (max absorption), nm	320	320

3.2. Degradation of cefazolin antibiotics

In the present research, the photocatalytic degradation of cefazolin antibiotics was studied on a TiO₂ nanoparticles-coated fixed bed treated with two light sources of UV_C (250 nm) and solar light. To determine the concentration of cefazolin by HPLC, the standard concentrations (5–25 mg/L) were injected into the device and the chromatogram peaks of cefazolin formed at a retention time of 1.2 min were recorded. Calibration curves are shown in Figs. 4a and b.

After this step, the test samples were injected to HPLC to determine the remaining concentration (Table 2). The highest

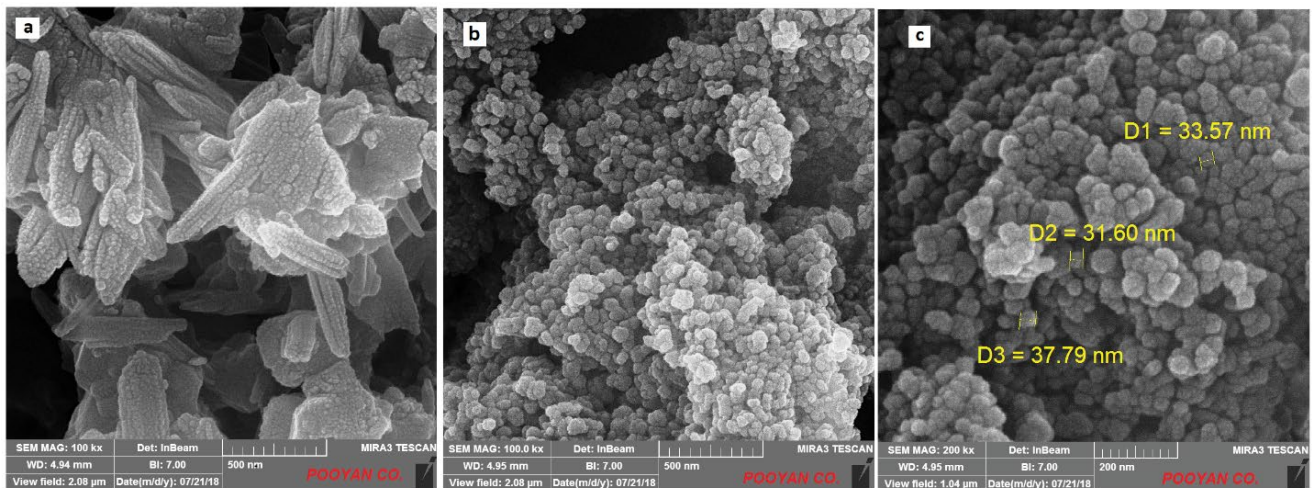


Fig. 3. FE-SEM surface of the glass substrate before coating (a) and after coating with TiO₂ (b,c).

Table 2

Main results of the tests presented in the experimental section

Time	Reactor 1							Reactor 2					
	C_0 (mg/L)	TiO ₂ /UV _C		UV _C		Syn%	R^2	TiO ₂ /Solar light		Solar light		Syn%	R^2
		C (mg/L)	k	C (mg/L)	k			C (mg/L)	k	C (mg/L)	k		
0	10	10	0	10	0	0		10	0	10	0	90	
5	10	7.8	0.05	9.9	0.002	96	0.98	8.9	0.02	9.9	0.002	93	0.99
10	10	5.1	0.07	9.6	0.004	94	0.99	7.1	0.03	9.8	0.002	93	0.99
15	10	2.12	0.16	9.3	0.005	97	0.99	6.3	0.03	9.8	0.001	96	0.99
20	10	0.8	0.13	9.1	0.005	97	0.99	5.6	0.03	9.8	0.001	96	0.99
25	10	0.53	0.12	9	0.004	97	0.98	4.1	0.04	9.7	0.001	98	0.98
30	10	0.4	0.11	8.8	0.004	96	0.99	3.2	0.04	9.7	0.001	98	0.98
60	10	0.2	0.06	8.1	0.003	95	0.99	2.7	0.02	9.6	0	99	0.98
90	10	0.1	0.05	7.7	0.003	94	0.98	2.1	0.02	9.6	0	99	0.98
120	10	0.1	0.04	7.3	0.002	94	0.99	1.8	0.01	9.6	0	99	0.98

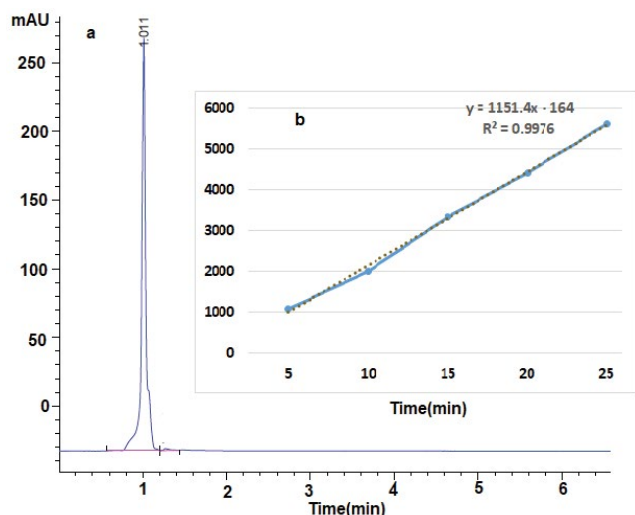


Fig. 4. Chromatogram peaks of cefazolin (a) and calibration curves (b).

efficiency of contaminant removal (i.e., 995) is observed in Reactor 1. In Reactor 2, the highest removal efficiency is 80%, which occurred after exposure to solar light for 120 min. The effect of UV_C and solar light was investigated using no catalyst. In this state, the highest removal efficiency for the UV lamp was 16%, and after being exposed to solar light, a removal rate of 3% was obtained. The simultaneous use of nanoparticles with any light source indicates that over 98% of the synergistic effect is obtained in this photocatalytic process (Table 2).

Fig. 5 presents the kinetic reaction of cefazolin at a concentration of 10 mg at different times. The results show that when UV (250) is in contact with TiO₂ nanocatalyst, more catalytic degradation occurred. This increase in the degradation of the contamination results from the production of reactive OH[•] radicals, which is a strong oxidizing agent.

As shown in Table 1, the most TiO₂ nanoparticle absorption is in a UV wavelength of 250 nm, which leads to cavitation and electron released from the nanoparticle and creates Rhodax reaction on the catalyst surface [11].

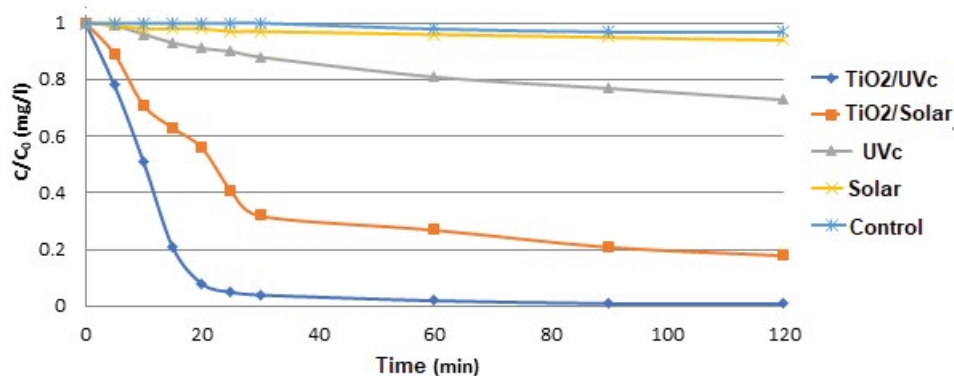


Fig. 5. Kinetics of the photocatalytic degradation of cefazolin.

These reactions create free radicals of oxygen in the solution. These molecules of oxygen tend to be absorbed by water molecules and produce OH[•] radicals [20]. In this photocatalytic process, in addition to OH[•], which plays an important role in the degradation of contaminants, other generated molecules such as O₂ and H₂O₂ may be effective in decomposing contaminants [21].

3.3. Solar light

Although the rate of cefazolin degradation in Reactor 2 (i.e., 81%) is lower than that in Reactor 1, this amount of contaminant degradation is considerable. As shown in Table 1, the light absorption of nanoparticles is higher in the wavelength range of 320 to 380 nm, which is the UV_A wavelength range of the sun.

Moreover, it can cause generating electrons and cavities on the catalyst surface, as well as OH[•] free radicals in Reactor 1. The reason for reducing the degradation efficiency in Reactor 2 than the Reactor 1 can be a reduction in light absorption at wavelengths more than 320 nm on the catalyst surface, as well as the reduction of the sun's UV intensity than the UV produced by the 10-watt argon lamp [22,23]. However, due to the geographical area of Damghan, which receives 871.1 h of solar light in the spring, the use of solar light with this efficiency may provide remarkable results (Fig. 6). From an economic point of view, in Reactor 1, in addition to the cost of purchasing a UV lamp which costs between \$20 and \$40 in Iran, as well as electricity consumption charge to produce UV from a 10-watt lamp, the cost of water purification is higher than that in Reactor 2. This makes the use of Reactor 2 more efficient using the natural light source.

3.4. TOC analysis

The results of this study were analyzed by GC-MS and TOC meters to determine the intermediate and by-product materials in the mineralization process during the photocatalytic process. These results are presented in Table 3. The results of the TOC test (Table 3) show that the mineralization process started from 19% in 5 min and reached 80% in 90 min and 86% at the end of the 120 min. However, removing pollutants started in 5 min with an efficiency of

Table 3
Process of mineralization and degradation during the photocatalytic process

Time (min)	C_0 (mg/L)	TiO_2/UV_c					$TiO_2/Solar\ light$				
		Degradation		TOC		R^2	Degradation		TOC		R^2
		C (mg/L)	%	C (mg/L)	%		C (mg/L)	%	C (mg/L)	%	
0	10	10	0	9.7	0		10	0	9.8	0	
5	10	7.8	22	8.1	19	0.98	8.9	11	9.2	8	0.97
10	10	5.1	49	7.4	30	0.98	7.1	29	8.4	16	0.96
15	10	2.12	79	6.8	32	0.99	6.3	37	8	20	0.98
20	10	0.8	92	5.82	62	0.99	5.6	44	7.4	26	0.98
25	10	0.53	95	5.61	64	0.99	4.1	59	6.6	34	0.97
30	10	0.4	96	5.32	57	0.99	3.2	28	5.9	41	0.97
60	10	0.2	98	2.1	79	0.98	2.7	79	3.6	64	0.97
90	10	0.1	99	1.98	80	0.99	2.1	82	3.2	68	0.98
120	10	0.1	99	1.4	86	0.98	1.8	84	3	70	0.97

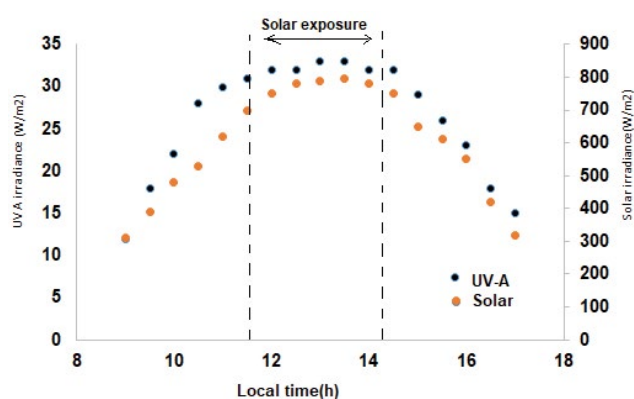


Fig. 6. Graphic representations of the values of solar UV and solar irradiance radiations registered during the degradation.

19%, reached the maximum elimination of 99% in 90 min, and remained up to 99% of efficiency until 120 min, leading to almost 100% degradation of the cefazolin [24].

3.5. GC-MS analysis

In the GC-MS test, samples of the reactors were extracted at times 30, 60, and 120 min. Compounds that were possibly created by the degradation of cefazolin were detected by the GC-MS test (Fig. 7). The molecular structure of these compounds is shown in Table 4. The samples were assigned with numbers of 1 to 12.

3.5.1. By-products after 30 min exposure

The chemical structure of cefazolin consists of B-lactate, carboxyl, and amide groups [4]. OH^\bullet free radicals created in the photocatalytic process can cause breaking structures between the C–H, C–N, C–S, O–C bonds. As shown in Table 4 and Fig. 7, in the first 30 min of the reaction, after

the structural breakdown of the contaminant, materials such as (1) 1-(1,3-thiazol)-1H, (2) propylthiouracil, (3) 1H-tetrazole and (4) 3H-1,2-dithiol-3-one, 4-methyl still were preserved in the circular structure. The structure of these compounds is shown in Fig. 7 (GC-MS) and Table 4 (molecular structure).

Researchers have studied the degradation of two intermediates used for the synthesis of cefazolin, namely 5-methyl-1,3,4 thiadiazole-2-methylthiol, and 5-methyl-1,3,4-thiadiazole-2-thiol, by UV/ H_2O_2 [25].

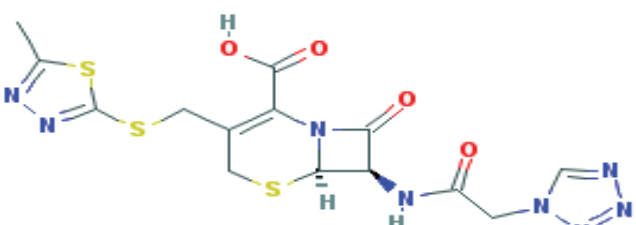
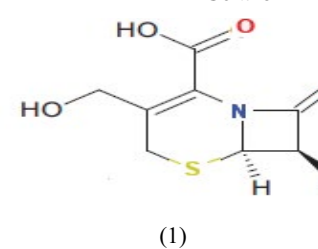
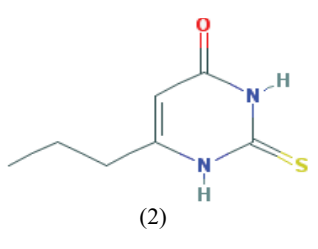
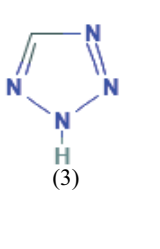
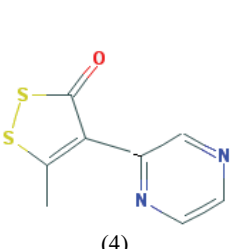
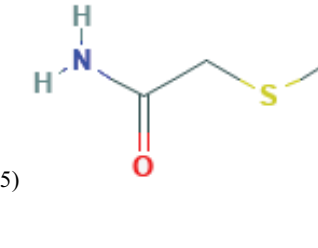
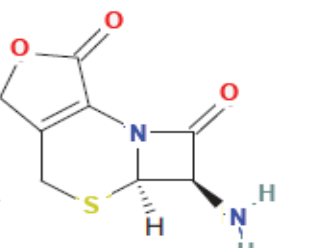
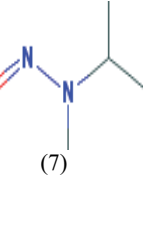
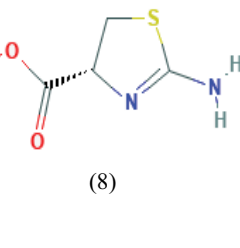
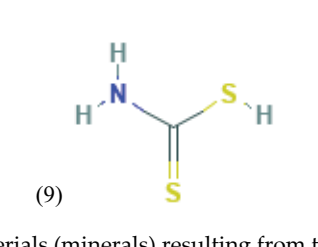
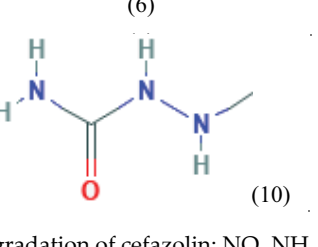
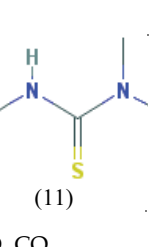
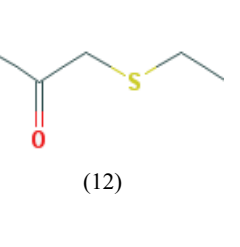
3.5.2. By-products after 60 min exposure

After 60 min, the materials in contact with free radicals are broken down and form a simpler material that contains mostly (5) 2-(Methylthio), (6) 5-(2-methyl-1,3-thiazol), (7) 2-Propanamine, N-ethyl-N-nitroso, and (8) 2-Aminothiazoline-4-carboxylic acid. The structure of these materials is shown in Fig. 7 and Table 4. Similar studies carried out on cefazolin degradation using the TiO_2/UV method show that free radicals of OH^\bullet produced by photocatalytic reactions can break large molecular structures and convert them to materials such as decarboxylation. The experimental results reported for cephalosporin antibiotics confirm this finding. Thus, it might be predicted that the dihydrodiazepin ring disappears when the β -lactam ring was opened [25].

3.5.3. By-products after 120 min exposure

After 60 min, the materials in contact with free radicals are broken down and form a simpler material that contains most of (9) thiocarbamic acid, (10) dithiocarbamic acid, (11) thiourea, trimethyl, and (12) 2-Propanone, 1-(ethylthio). The structure of these compounds is shown in Fig. 7 and Table 4. Subsequently, the circular structure of these compounds is further converted to simpler materials in contact with OH^\bullet . These researchers interpreted the reaction mechanism in relation to the photogenerated OH^\bullet radicals and concluded that the two compounds are

Table 4
Molecular structure compounds that were possibly created by the degradation of cefazolin in GC-MS test

Time (min)	Products
0	
30	 (1)  (2)  (3)  (4)
60	 (5)  (6)  (7)  (8)
120	 (9)  (10)  (11)  (12)

Inorganic materials (minerals) resulting from the degradation of cefazolin: NO_3 NH_3 SO_4 CO_2 [4]

completely converted to by-products that undergo further degradation with the breaking of the thiadiazole ring. Finally, these molecules become more stable by turning to minerals containing sulfate nitrate and ammoniac compound following the oxidation. According to the results of the TOC test, 86% of the cefazolin is converted to mineral compounds such as carbon dioxide, sulfates, and nitrates, and the remaining 14% turns into an intermediate organic mineral, most likely propanone and thiocarbamic acid [4]. The results compared with those of this study, which are presented in the form of the GC graph, shows materials such as (1), (3), (6), and (8) are consistent with those reported in the current research. Also, Gurkan et al. found that OH^\bullet molecules tend to attack the sulfur structure in the cefazolin molecule such that by breaking these bonds, stable compounds including sulfates, nitrates, and ammonia are produced [26].

4. Conclusion

It can be said that a TiO_2 nanoparticle bed can produce a catalytic surface for the photocatalytic process with a coating on the glass substrate. Both natural and artificial UV light sources are capable of generating electrons and cavities at the catalyst surface and then creating free radicals such as OH^\bullet . Free radicals initially show a high tendency to react with the molecular structure of Cefazolin and turn it into the circular intermediate substance, and then the loops open turning in to simpler structures. Ultimately, in the vicinity of OH^\bullet , these materials convert to minerals such as sulfates nitrates, and ammonia. In general, it can be said that the Reactor 1 is capable of eliminating cefazolin from the water with efficiency above 99% and using a natural light source, Reactor 2 can withstand 80% of efficiency without consuming any artificial energy source for eliminating Cefazolin from aquatic environments with much lower costs.

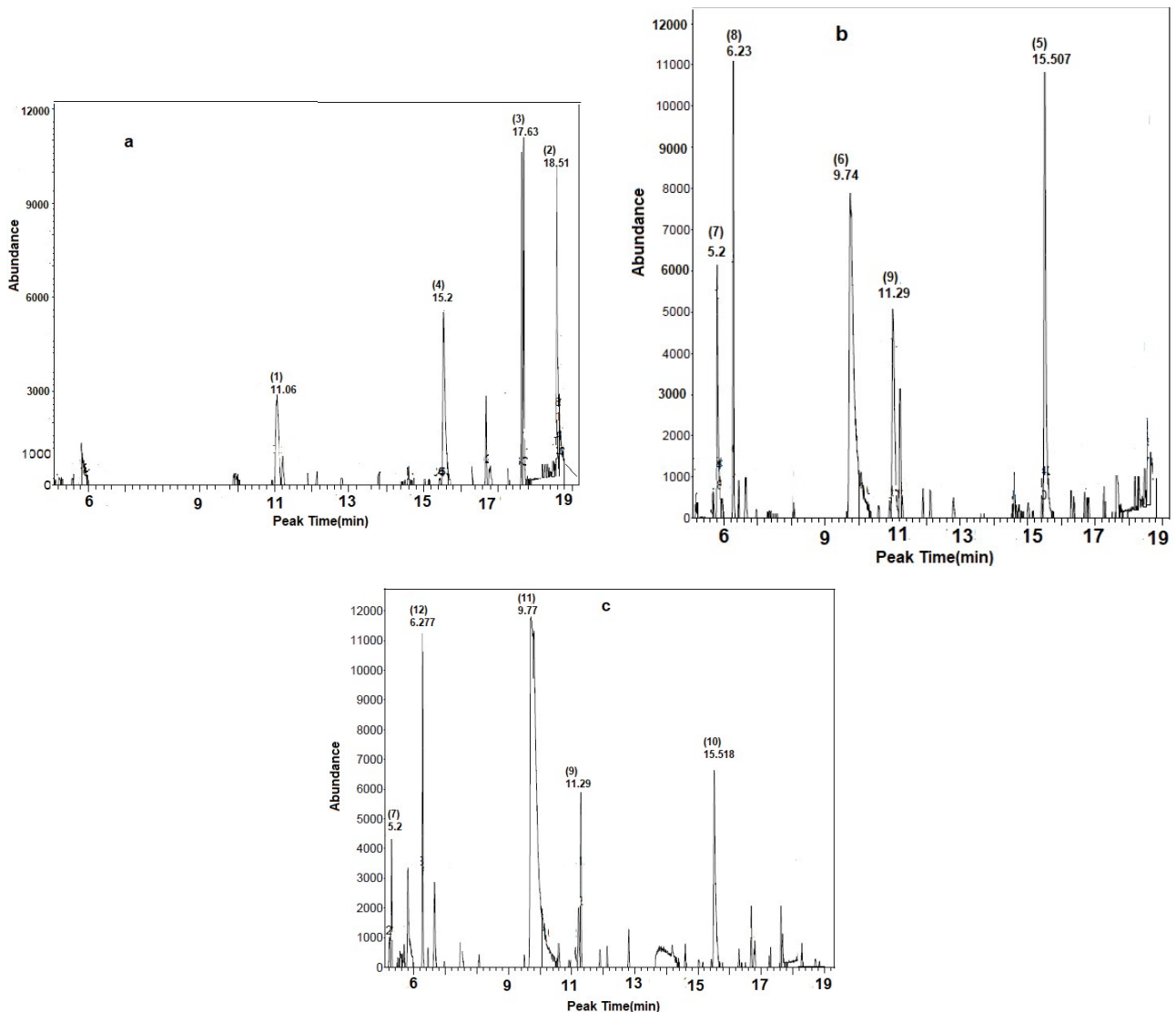


Fig. 7. GC-MS chromatogram of the degradation of cefazolin, after 30 min exposure (a), after 60 min exposure (b), after 120 min exposure (c).

References

- [1] E.S. Elmolla, M. Chaudhuri, Comparison of different advanced oxidation processes for treatment of antibiotic aqueous solution, *Desalination*, 256 (2010) 43–47.
- [2] K. Ikehata, N. Jodeiri Naghashkar, M. Gamal El-Din, Degradation of aqueous pharmaceuticals by ozonation and advanced oxidation processes: a review, *Ozone Sci. Eng.*, 28 (2006) 353–414.
- [3] R. Molinari, F. Pirillo, V. Loddo, L. Palmisano, Heterogeneous photocatalytic degradation of pharmaceuticals in water by using polycrystalline TiO_2 and a nanofiltration membrane reactor, *Catal. Today*, 118 (2006) 205–213.
- [4] Y.Y. Gurkan, N. Turkten, A. Hatipoglu, Z. Cinar, Photocatalytic degradation of cefazolin over N-doped TiO_2 under UV and sunlight irradiation: prediction of the reaction paths via conceptual DFT, *Chem. Eng. J.*, 184 (2012) 113–124.
- [5] H.-S. Son, G. Ko, K.-D. Zoh, Kinetics and mechanism of photolysis and TiO_2 photocatalysis of triclosan, *J. Hazard. Mater.*, 166 (2009) 954–960.
- [6] M. Ahmadi, H. Rahmani, A. Takdastan, N. Jaafarzadeh, A. Mostoufi, A novel catalytic process for degradation of bisphenol A from aqueous solutions: a synergistic effect of nano- Fe_3O_4 @ Alg-Fe on $\text{O}_3/\text{H}_2\text{O}_2$, *Process Saf. Environ. Prot.*, 104 (2016) 413–421.
- [7] Y. Abdollahi, A.H. Abdullah, Z. Zainal, N.A. Yusof, Degradation of m-cresol with Mn doped ZnO nanoparticles under visible light irradiation, *Fresenius Environ. Bull.*, 21 (2012) 256–262.
- [8] Y. Jiao, W. Ge, R. Qin, B. Sun, W. Jiang, D. Liu, Influence of cadmium stress on growth, ultrastructure and antioxidative enzymes in *Populus 2025*, *Fresenius Environ. Bull.*, 21 (2012) 1375–1384.
- [9] M. Fazlzadeh, A. Rahmani, H.R. Nasehinia, H. Rahmani, K. Rahmani, Degradation of sulfathiazole antibiotics in aqueous solutions by using zero valent iron nanoparticles and hydrogen peroxide, *Koomesh*, 18 (2016) 350–356.
- [10] M. Tabatabaee, A. Ghotbifar, A.A. Mozafari, Photosensitized degradation of azo dyes on Fe, Ti, and Al oxides. Mechanism of charge transfer during the degradation, *Fresenius Environ. Bull.*, 21 (2012) 1468–1473.
- [11] M. Ahmadi, K. Rahmani, A. Rahmani, H. Rahmani, Removal of benzotriazole by photo-Fenton like process using nano zero-valent iron: response surface methodology with a Box-Behnken design, *Pol. J. Chem. Technol.*, 19 (2017) 104–112.

- [12] M. Farzadkia, K. Rahmani, M. Gholami, A. Esrafil, A. Rahmani, H. Rahmani, Investigation of photocatalytic degradation of clindamycin antibiotic by using nano-ZnO catalysts, *Korean J. Chem. Eng.*, 31 (2014).
- [13] M. Gholami, K. Rahmani, A. Rahmani, H. Rahmani, A. Esrafil, Oxidative degradation of clindamycin in aqueous solution using nanoscale zero-valent iron/H₂O₂/US, *Desal. Wat. Treat.*, 57 (2016) 13878–13886.
- [14] K. Sivagami, R.R. Krishna, T. Swaminathan, Photo catalytic degradation of pesticides in immobilized bead photo reactor under solar irradiation, *Sol. Energy*, 103 (2014) 488–493.
- [15] K. Sunada, T. Watanabe, K. Hashimoto, Studies on photokilling of bacteria on TiO₂ thin film, *J. Photochem. Photobiol.*, 156 (2003) 227–233.
- [16] J.J. Feng, Q.-C. Liao, A.-J. Wang, J.-R. Chen, Mannite supported hydrothermal synthesis of hollow flower-like ZnO structures for photocatalytic applications, *Cryst. Eng.*, 13 (2011) 4202–4210.
- [17] S. Sato, R. Nakamura, S. Abe, Visible-light sensitization of TiO₂ photocatalysts by wet-method N doping, *Appl. Catal.*, 284 (2005) 131–137.
- [18] A. Emeline, G. Kuzmin, N. Serpone, Wavelength-dependent photostimulated adsorption of molecular O₂ and H₂ on second generation titania photocatalysts: the case of the visible-light-active N-doped TiO₂ system, *Chem. Phys. Lett.*, 454 (2008) 279–283.
- [19] A.V. Emeline, V.N. Kuznetsov, V.K. Rybchuk, N. Serpone, Visible-light-active titania photocatalysts: the case of N-doped s—properties and some fundamental issues, *Int. J. Photoenergy*, 2008 (2008), <https://doi.org/10.1155/2008/258394>.
- [20] A. Bozzi, A. Lopez, G. Mascolo, G. Tiravanti, Pharmaceuticals degradation by UV and UV/H₂O₂ treatments, *Water Sci. Technol. Water Supply*, 2 (2002) 19–26.
- [21] A. Lopez, A. Bozzi, G. Mascolo, J. Kiwi, Kinetic investigation on UV and UV/H₂O₂ degradations of pharmaceutical intermediates in aqueous solution, *J. Photochem. Photobiol.*, 156 (2003) 121–126.
- [22] A. Yazdanbakhsh, A. Rahmani, M. Massoudinejad, M. Jafari, M. Dashtdar, Accelerating the solar disinfection process of water using modified compound parabolic concentrators (CPCs) mirror, *Desal. Wat. Treat.*, 57 (2016) 23719–23727.
- [23] H. Rahmani, A. Rahmani, M. Yousefi, K. Rahmani, Degradation of sulfamethoxazole antibacterial by sono-Fenton process using nano-zero valent iron: influence factors, kinetic and toxicity bioassay, *Desal. Wat. Treat.*, 150 (2019) 220–227.
- [24] A. Rahmani, A. Asadi, A. Fatehizadeh, A.R. Rahmani, M.R. Zare, Interactions of Cd, Cr, Pb, Ni, and Hg in their effects on activated sludge bacteria by using two analytical methods, *Environ. Monit. Assess.*, 191 (2019) 124.
- [25] Y. Okamoto, K. Kiriya, Y. Namiki, J. Matsushita, M. Fujioka, T. Yasuda, Degradation kinetics and isomerization of cefdinir, a new oral cephalosporin, in aqueous solution, *J. Pharm. Sci.*, 85 (1996) 976–983.
- [26] M.R. Zare, M. Amin, M. Nikaeen, M. Zare, B. Bina, A. Fatehizade, A. Rahmani, M. Ghasemian, Simplification and sensitivity study of Alamar Blue bioassay for toxicity assessment in liquid media, *Desal. Wat. Treat.*, 57 (2016) 10934–10940.